INAEME: Integral Neoantigen Analysis with Entirety of Mutational Events

Vladimir Kovacevic, School of Electrical Engineering, University of Belgrade
Nevena M. Ilic Raicevic, Velsera, Charlestown, MA
Ognjen S. Milicevic, Faculty of Medicine, University of Belgrade

Abstract
Neoantigens are peptides on the surface of cancer cells presented to the immune system. Multiple novel therapeutic approaches involve the identification and administration of neoantigens to trigger immunity-induced tumor regression. Here, we present the novel, integral bioinformatic analysis workflow for neoantigen discovery, denoted INAEME (Integral Neoantigen Analysis with Entirety of Mutational Events). The workflow performs integral processing of an individual's DNA tumor-normal and RNA tumor raw reads in order to output prioritized neoantigen candidates. Our evaluation analysis includes a wide scope of mutational events so far not considered in the existing solutions, including phasing of variants, influence of both somatic and germline variants, positions of all transcripts, neighboring variants, and frameshifts. The influence of each mutational event on the accuracy of predicted neoantigen candidates is tested across 300 TCGA samples from multiple cancer types. The obtained results have demonstrated the significance of considering the entirety of mutational events to obtain an accurate set of strong neoantigen candidates for cancer immunotherapy targets or vaccines.

Introduction

Every cell in our body has mechanisms to cleave discarded endogenously-synthesized proteins and present some of their fragments on its surface as antigens. If the antigen originates from mutated DNA it is called neoantigen and it represents the unique identifier of cancer cells. Our immune system's T-cells recognize them and annihilate thousands of cancer cells every day [1]. Still, cancer cells develop molecular mechanisms and signals that sometimes enable them to elude the immune system [2][3][4] and continue to grow and metastasize to other tissues. The concept of boosting and training the immune system resulted in multiple novel immunotherapeutic approaches that involve identifying neoantigens and using them to trigger immunity-induced tumor regression [5][6][7][8][21][22]. The main requirement for identifying neoantigens is the availability of genomic sequences originating from both tumor and normal (wild type) tissues. These two sequences are compared to identify the positions of somatic variants, which create alternations of amino acids. Protein sequences translated from positions around altered amino acids represent neoantigen candidates. For this purpose, a number of bioinformatic analyses (workflows) for neoantigen discovery using NGS data have been developed [9][10][11][12][13][14][15]. The differences between solutions mostly lie in

bioinformatic tools being used and mutational events that are considered. Mutational events include any modification of the reference genome during the application of the called variants necessary to obtain the exact nucleotide or protein sequence from the individual. One of the first publicly available solutions was pVACseq [9]. Initially, it considered only the modifications of the reference genome from single nucleotide variations, while later versions also considered indels, but not the influence of proximal (neighboring) variants. pVACSeq workflow starts from already reconstructed variants and its structure is not described in any of the existing workflow description languages which would make it portable and reproducible [18]. The influence of RNA expression is taken into account, but not the RNA variant calling for determining whether the expressed transcript of the given allele is a reference or alternative (with variant). pVACSeq supports a wide variety of MHC Class I and MHC Class II binding prediction tools. The next solution, CloudNeo workflow [10] is described in Common Workflow Language (CWL). It also starts from reconstructed variants but does not consider RNA expression influence. PGV [11]is an integral solution taking into account the influence of indels, proximal variants, and RNA expression, but not supporting custom gene annotation file and the influence of frameshifts from neighboring indels. Proximal variant correction (PVC) workflow [12] provides integral analysis with an emphasis on considering the influence of close variants. The authors don't take into account the influence of transcript positions and frameshifts stating that it is substantially complicated to consider the context of transcriptome coordinates since intronic coordinates must be ignored when scanning upstream and downstream [12]. The mentioned features and mutational events not covered in the existing solutions produced the need for creating Integral Neoantigen Analysis with the Entirety of Mutational Events (INAEME). Table 1 lists the supported features and mutational events in publicly available Neoantigen workflows and INAEME, our proposed solution.

Feature or mutational event	INAEME	pVACSeq	CloudNeo	PGV	PVC
Indels	+	+	+	+	-
Proximal (neighboring) variants	+	-	-	+	+
Frameshift created by proximal indels	+	-	-	-	-
Variant phasing	+	-	-	+	+
Custom gene/transcript annotations, excluding introns, backward and forward strands	+	-	-	-	-
Integral analysis (from FASTQ to scored neoantigens)	+	-	-	+	+
RNA expression	+	+	-	+	-
RNA variant calling	+	-	-	-	-

Described in a workflow description language	+	-	+	+	-

Table 1: List of neoantigen detection features or mutational events present in four publicly available algorithms (pVACSeq, CloudNeo, PGV, PVC) and our proposed solution (INAEME).

Figure 1a shows an example of applying a variant to the reference genome to produce a neoantigen candidate. We considered only non-synonymous somatic variants in the gene's coding regions and ignored synonymous and intron-falling variants. The DNA chain of nucleotides is transcribed to mRNA which is, after splicing, translated to protein. For better referencing, the short protein sequence around altered amino acid(s) will be called the neoantigen nest. A peptide extracted from a neoantigen nest that contains altered amino acid(s) is called a neoepitope. Neoepitope paired with independently calculated individual's HLA Class 1 type forms a neoantigen candidate.

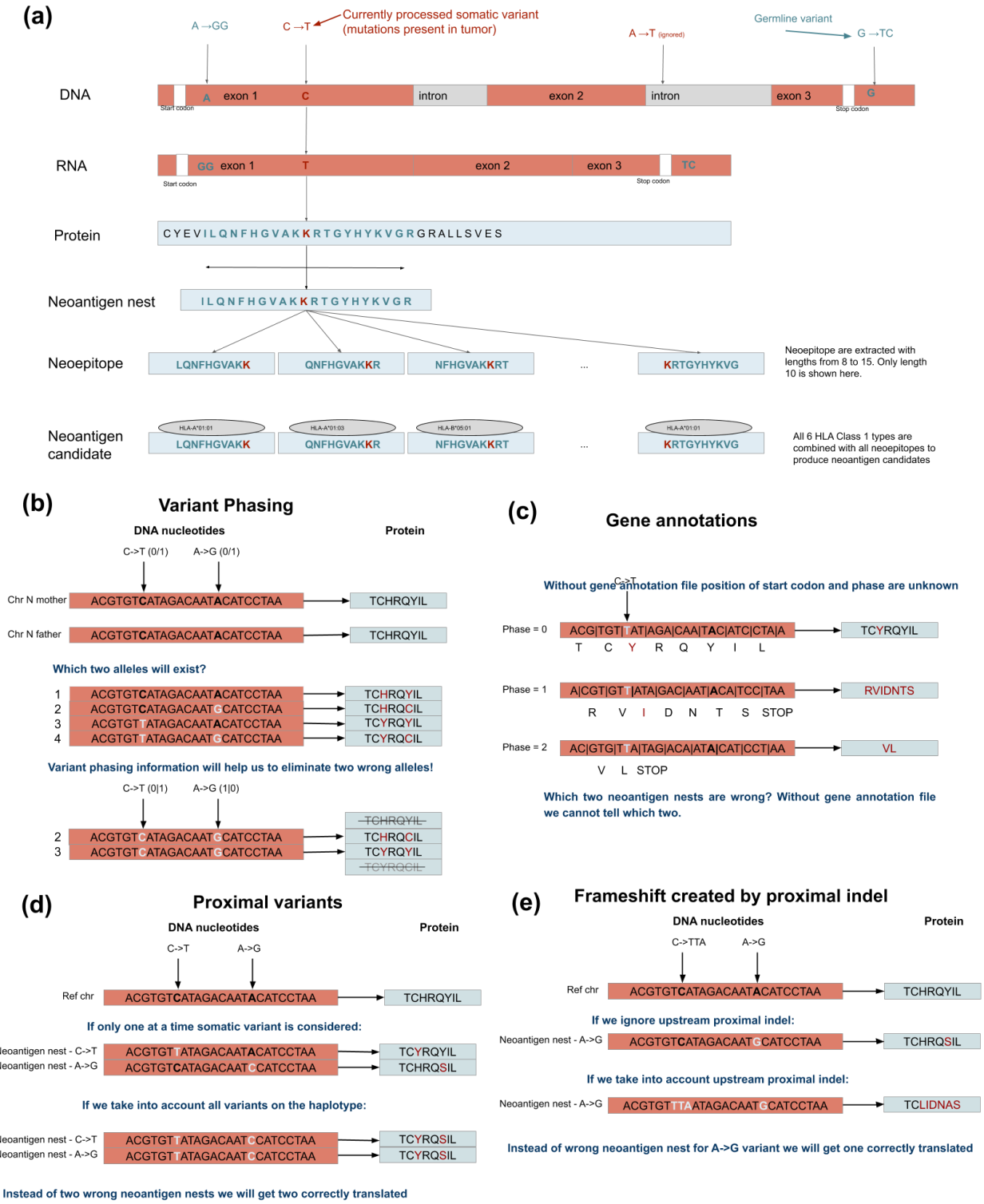

Figure 1: (a) Illustration of the mutational event with somatic and germline variants and their influence on protein sequence, followed by extraction of neoantigen nest from the protein, slicing neoepitopes, and creating neoantigen candidates by combining all calculated HLA types to all neoepitopes. (b) Variant phasing information enables us to determine whether variants fall

on the same haplotype. If it is available it is possible to exclude nonexistent neoantigen nests. (c) Custom gene annotation file enables correct starting position and phase for translating nucleotide sequence to protein (d) Proximal variants influence alters neoantigen nest (e) Frameshift created by proximal indel can almost completely alter the neoantigen nest.

Disregarding some of the mutational events can lead to the identification of different (incorrect) neoantigen nest which further spawns incorrect neoantigen candidates. For example, ignoring indels obviously creates incorrect DNA sequence on their positions, but also does not take into account the influence of variant phasing (determines and groups variants belonging to the same haplotype), neighboring (proximal) variants, frameshifts created by proximal indels and usage of custom gene annotation file will also lead to obtaining incorrect neoepitopes in neoantigen candidates. Figures 2b-e illustrate and explain the influence of these four mutational events. In the experiments presented in this paper, we measured the influence of variant phasing, proximal variants, and frameshifts from proximal variants, while measuring the impact of gene annotations usage (positions of the start codon and phase shift) illustrated in Figure 1e is skipped since only one-third of the discovered neoantigen candidates could be correct.

Results

In order to demonstrate the benefits of considering the entirety of mutational events (alternations of the reference genome and thus, the proteins caused by gene variants during the reconstruction of the individual's genome), we processed with INAEME neoantigen discovery workflow 300 samples from The Cancer Genome Atlas (TCGA) [16] containing tumor and normal DNA reads. Additionally, seven different configurations of INAEME that exclude some of the mentioned mutational events were run giving a total of 2400 analyses (tasks) executed on the Cancer Genomics Cloud platform [17]. The execution time of neoantigen discovery per sample on AWS computational cloud instance (c5.4xlarge - 16 processors and 32 GB of memory) varies between 2 and 12 hours, depending on the cancer type and mutational burden (Figure 2 in Supplementary). The samples used in the analysis are selected from three different tumor types as used in PVC [12]: 100 cases of melanoma, hepatocellular carcinoma, and lung squamous cell carcinoma. On these selected samples we measured the differences in obtained neoantigen nests and neoepitopes when some of the mutational events were not considered. Mutational events investigated here include indel variants, the influence of proximal indels, phasing, and window size around variants to look for proximal variants. We also measured the influence of ignoring one or more mutational events in current publicly available neoantigen discovery algorithms. We made INAEME flexible to allow "switching off" the selected mutational events in order to measure the exact consequence of neglecting one or more of them as in the publicly available algorithms. The consequence of neglecting mutational events is the appearance of falsely detected (FD) and falsely excluded (FE) neoantigen nests and neoepitopes. We will use in the rest of the paper FD and FE terms to distinguish candidates wrongly appeared or incorrectly lost due to neglecting some of the mutational events. Candidates that appear in both scenarios, with and without the exclusion of mutational event(s)

we will call correctly detected (CD). Figure 2a shows neoantigen nests comparison across three cancer types, the counts of correctly detected and the distributions of FD and FE appeared when one or more of these mutational events is switched off, respectably: all indels are ignored, the proximal area size of only 89 nucleotides as used in PVC, all proximal variants ignored (the proximal area around variant equals zero), excluding variant phasing (phasing off) and influence of indels around currently processed somatic variant. Figure 2a also shows the comparison of INAEME when all mutational events are considered with INAEME with excluded mutational events (EME) as in publicly available algorithms: PGV (excludes ignore neighboring indels - PGV-EME), pvacseq, and CloudNeo (both exclude phasing and all neighboring variants - pvacseq&CloudNeo-EME) and PVC (exclude indels and have a proximal area of 89 nucleotides - PVC-EME). Figure 2b shows precision, recall, and f-scores for the same listed mutational events exclusion and algorithms also compared to the algorithm where the entirety of mutational events are taken into consideration. FD, FE, and CD distributions and precision, recall, and f-score for neoepitopes are very similar to neoantigen nests' distribution which makes sense since they are derived from them. They are given in Figure 1 of supplementary material for completeness of the reported data.

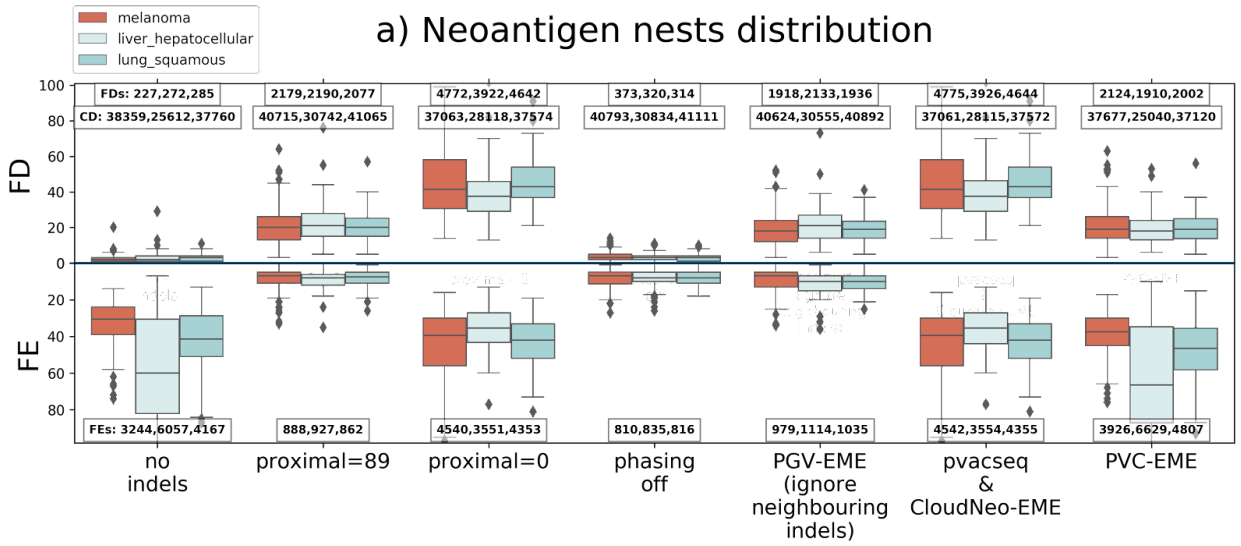
a) Neoantigen nests distribution
melanoma
liver_hepatocellular
lung_squamous
FD
FE
FDs: 227,272,285
CD: 38359,25612,37760
2179,2190,2077
40715,30742,41065
4772,3922,4642
37063,28118,37574
373,320,314
40793,30834,41111
1918,2133,1936
40624,30555,40892
4775,3926,4644
37061,28115,37572
2124,1910,2002
37677,25040,37120
FEs: 3244,6057,4167
888,927,862
4540,3551,4353
810,835,816
979,1114,1035
4542,3554,4355
3926,6629,4807
no indels
proximal=89
proximal=0
phasing off
PGV-EME (ignore neighbouring indels)
pvacseq & CloudNeo-EME
PVC-EME

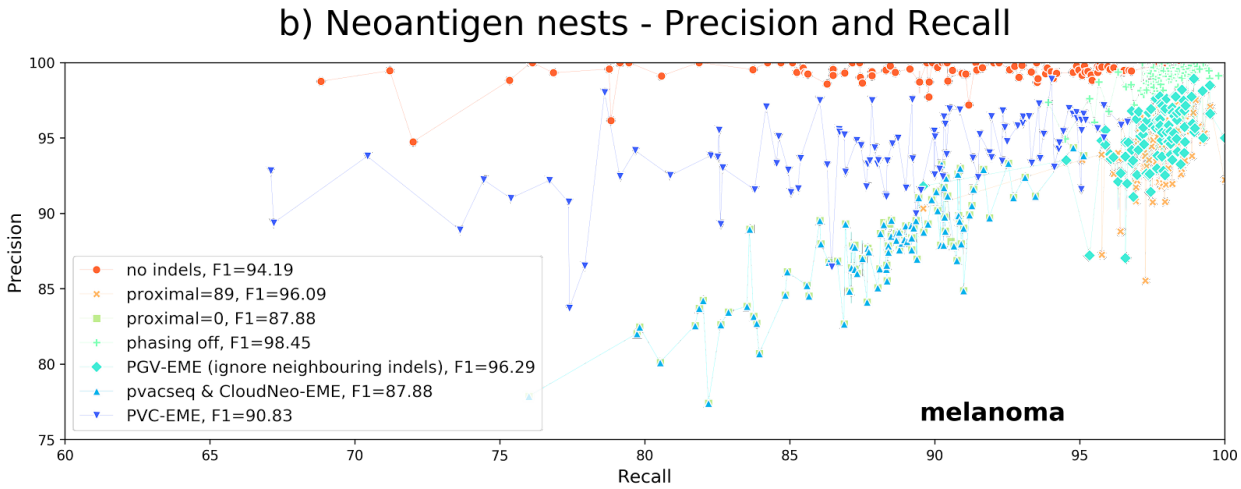
b) Neoantigen nests - Precision and Recall
Precision
Recall
no indels, F1=94.19
proximal=89, F1=96.09
proximal=0, F1=87.88
phasing off, F1=98.45
PGV-EME (ignore neighbouring indels), F1=96.29
pvacseq & CloudNeo-EME, F1=87.88
PVC-EME, F1=90.83
melanoma

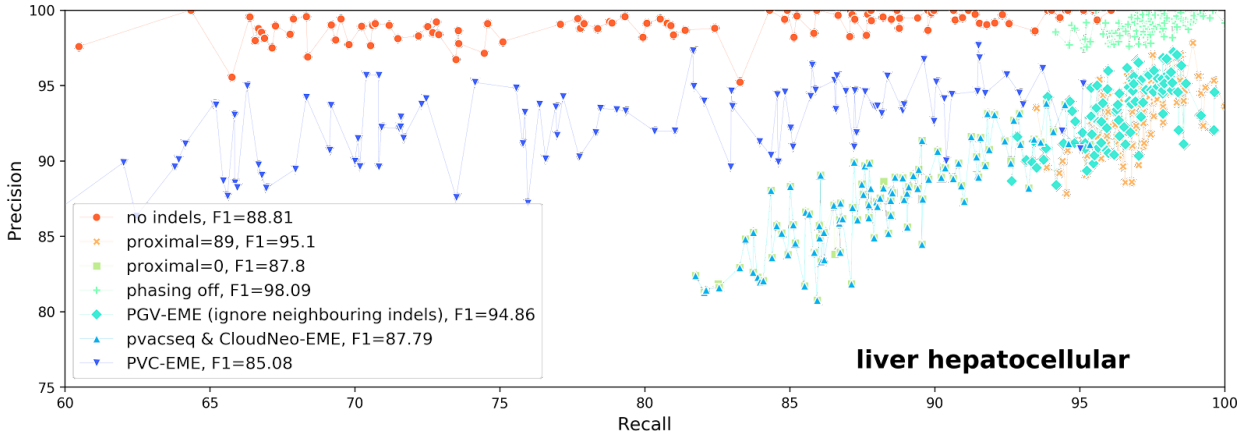
Precision
Recall
no indels, F1=88.81
proximal=89, F1=95.1
proximal=0, F1=87.8
phasing off, F1=98.09
PGV-EME (ignore neighbouring indels), F1=94.86
pvacseq & CloudNeo-EME, F1=87.79
PVC-EME, F1=85.08
liver hepatocellular

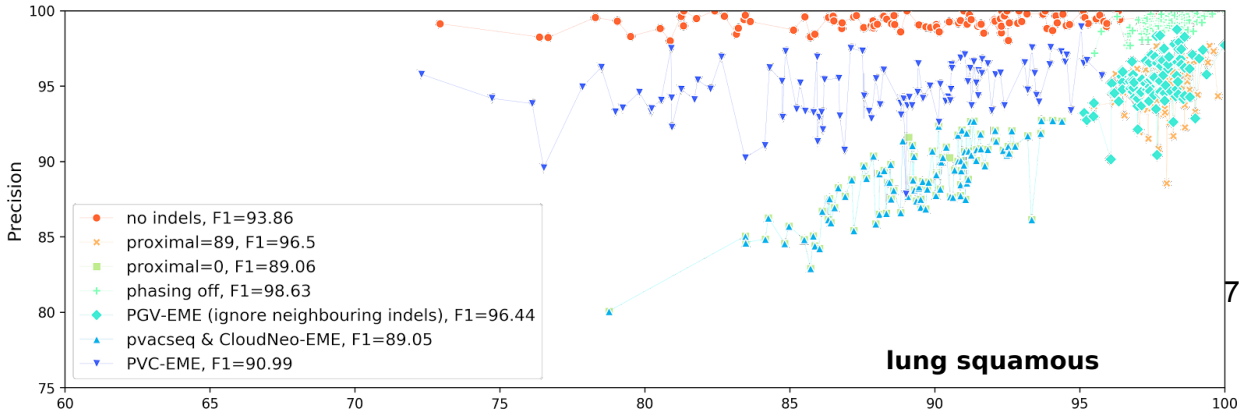
Precision
no indels, F1=93.86
proximal=89, F1=96.5
proximal=0, F1=89.06
phasing off, F1=98.63
PGV-EME (ignore neighbouring indels), F1=96.44
pvacseq & CloudNeo-EME, F1=89.05
PVC-EME, F1=90.99
lung squamous

Figure 2: (a) Distribution of falsely discovered (FD), falsely excluded (FE), and correctly detected (CD) neoantigen nests across 100 samples of melanoma, hepatocellular carcinoma, and lung squamous cancer, when some of the mutational events are switched off: all indels are ignored, the proximal area size of only 89 nucleotides as used in PVC, all proximal variants ignored (proximal=0), excluding variant phasing (phasing off), the influence of indels around currently processed somatic variant (as excluded in PGV - PGV-EME), pvacseq & CloudNeo - EME (excluding phasing and proximal area equals 0) and PVC-EME (no indels and proximal area of 89). Total numbers of FDs, FEs, and CDs are given in the boxes per cancer type for each mutational event switched off and for each algorithm with its mutational events switched off. (b) Precision and recall scores on neoantigen nests across 100 samples each of melanoma, hepatocellular carcinoma, and lung squamous cancer when the same mutational events are switched off. Mean f-scores (F1) across all samples when a mutational event is switched off are given in the figure's legend.

Next, we want to demonstrate the amounts of strong neoantigen candidates in falsely discovered and falsely excluded neoantigen candidates by measuring its major histocompatibility (MHC) binding affinity (the probability that neoepitope attached in MHC complex will be expressed at the surface of the antigen-presenting cell). For that purpose, we used three bioinformatic tools available in INAEME. First, we selected candidates with an agretopicity score (the difference between MHC binding scores of alternated peptide and its corresponding reference peptide) calculated by NetCTLPan [NetCTLPan] that is larger than 0.1 which could be considered significant. The mean per sample count of such candidates from FD and FE groups across three cancer types for several mutational events and algorithms is shown in Figure 3a-b. Next, for falsely discovered and falsely excluded neoantigen candidates, we showed the mean per sample count of candidates scored by NetCTLPan in the top 10% of all candidates (Figure 3c-d). The mean per sample count of FD and FE candidates with ic50 score smaller than 500 calculated by NetMHCpan [29] and PickPocket [30] are shown in Figure 3e-h, respectively. This threshold value for the ic50 score distinguishes strong neoantigen candidates [32].

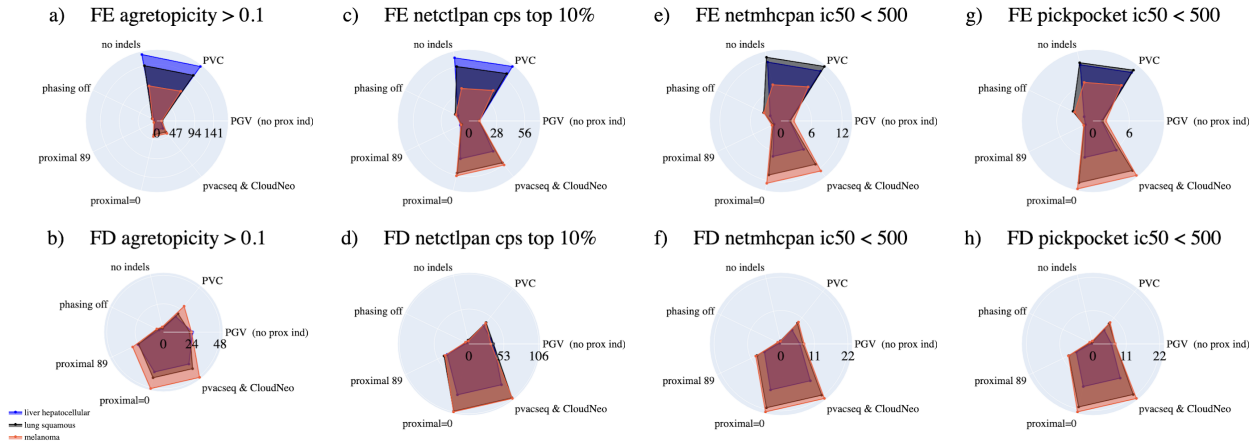

Figure 3: Mean per sample counts of strong neoantigen candidates across 300 TCGA samples of 3 cancer types for falsely excluded and falsely discovered neoantigen candidates with the exclusion of the single mutational events and exclusion of the mutational events from publicly available algorithms (radial axis). Mean count per sample of FE (a) and FD (b) neoantigen candidates with agretopicity larger than 0.1 calculated by NetCTLPan tool. Total 327 neoantigen candidates on average per sample with agretopicity > 0.1 were called without exclusion of any mutational event. Mean per sample count of FE (c) and FD (d) candidates within the top 10% NetCTLPan's combined prediction scores. Total 565 neoantigen candidates on the average per sample were within the top 10% scored by NetCTLPan called without exclusion of any mutational event. Mean per sample count of FE (e) and FD (f) candidates with ic50 < 500 calculated by NetMHCpan. A total of 114 neoantigen candidates on average per sample were with ic50<500 scored by NetMHCpan and called without exclusion of any mutational event. Mean per sample count of FE (g) and FD (h) candidates with ic50 < 500 calculated by PickPocket. Total 112 neoantigen candidates on average per sample were with ic50<500 scored by PickPocket and called without exclusion of any mutational event.

The largest stumbling block in the neoantigen discovery area is the lack of truthset samples with validated neoantigen candidates. For that reason, a fair comparison of accuracy between different neoantigen discovery algorithms can't be done. For that reason, we have decided to show in this paper the tests that measure the impact of selected mutational events and highlight the necessity for their inclusion in the neoantigen discovery algorithms. The first initiative to create a truthset and propose best practices in neoantigen discovery has been started through the Tumor Neoantigen Selection Alliance - TESLA challenges organized by the Parker Institute for Cancer Immunotherapy. INAEME has been tested throughout the last three rounds (Round 2, Round X, and Round 3) of the TESLA challenges. When analyzing 8 samples published in [19] having a total of 38 confirmed neoantigen candidates INAEME managed to detect and give high scores to 34 of them (Figure 4).

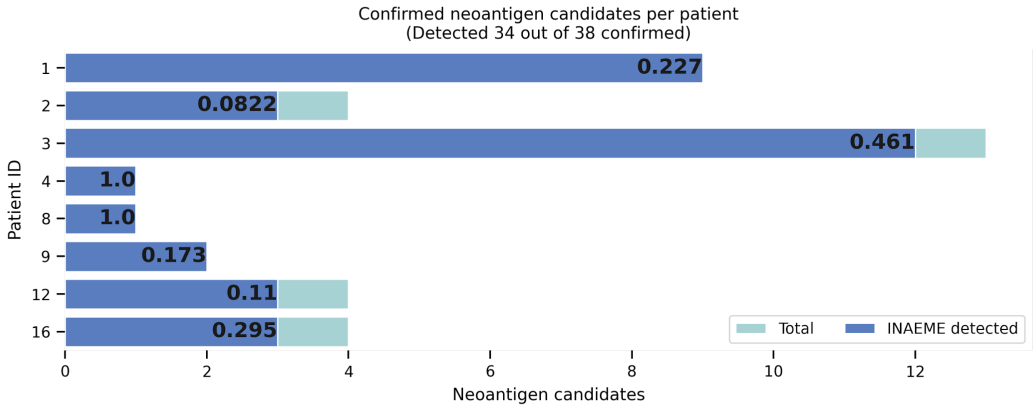

Figure 3: Flow cytometry and microscopy confirmed neoantigen candidates from [19] detected and scored by INAEME with AUPRC metric across 8 patients. INAEME final neoantigen prediction score was created by combining NetMHCPan IC50 score with weight 0.7 and RNA

expression score with weight 0.3. Neoantigen candidates were also filtered with the following criteria: NetCTLPan combined prediction score > 0.2 and tumor VAF > 0.1.

Discussion

The main idea behind developing and testing INAEME is to highlight and prove the significance of supporting the entirety of mutational events. Neglecting some strong-MHC-binding neoantigen candidates leads to lowering the chance of constructing an adequate cancer vaccine that targets existent neoepitopes on the surface of the cancerous cells. Cancer vaccines with a smaller number of neoantigens might not be as effective due to the mutational frequency of the tumor and the possible elimination of immunogenic tumor clones [33]. On the other hand, including some of the false neoantigen candidates, besides not targeting cancerous cells for destruction, increases the risk of provoking hazardous autoimmune reactions [34]. Our tests across 300 TCGA samples demonstrated a significant number of falsely called and missed neoantigen nests and candidates when neglecting some of the mutational events. As a summary, we compared INAEME (implemented with the entirety of mutational events) with the INAEME version with excluded mutational events from publicly available neoantigen discovery algorithms such as PGV, pvacseq, CloudNeo, and PVC. Our neoantigen discovery analysis showed 384 neoantigen nests (putative sources of neoantigen candidates) on average per sample. Across 300 TCGA samples, we obtained 20 (5.2%) incorrect and 10 missed (2.6%) neoantigen nests for PGV [11]on average per sample. For pvacseq [9] and CloudNeo [10] 44 (11.45%) were incorrect and 42 (10.93%) were missed and for PVC [12] 20 (5.2%) were incorrect and 51 (13.28%) missed (detailed distributions per cancer type are shown in Figure 2). We also tested MHC binding affinities for missed and falsely called neoantigen candidates and proved the existence of strong neoantigen candidates among them (Figure 3).
When comparing distributions of missed neoantigen nests between these 3 cancer types the noticeable difference when ignoring proximal variants (proximal=0) is around 1000 more FE neoantigen nests across all melanoma and lung squamous samples than on liver hepatocellular samples which could be explained by larger mutational burden present in these two cancer types [34].
Minimizing both FDs and FEs neoantigen nests is very important: FEs to avoid elimination of potentially correct neoantigen candidates and FDs to remove incorrect, potentially hazardous neoantigen candidates. From our results, the mutational event with the highest influence on FEs is ignoring indels and it eliminates on average 32.44 (8.45%) correct neoantigen nests on melanoma (f-score: 94.19), 60.57 (23.65%) on liver hepatocellular with f-score 88.81 and 41.67 (11.03%) on lung squamous with f-score 93.86 samples. The significance of indels in generating strong neoantigen candidates is proven in many studies such as [33] where results show that indels generate three times as many predicted neoantigen candidates as non-synonymous single nucleotide variants and nine times as many strong neoantigen candidates. A smaller number of indels than expected on the melanoma samples is due to a smaller proportion of indels in this cancer type. This result matches with findings in [33] where melanoma has the second smallest proportion of indels out of a total of 19 analyzed cancer types.

The second mutational event that highly influences the appearance of FEs is excluding proximal variants which creates on average 45.40 (12.25%) FEs in melanoma, 35.51 (12.63%) on the liver, and 43.53 (11.58%) on lung cancer samples.
Ignoring proximal variants also creates the largest number of FDs across all 3 cancer types: 47.72 (12.87%) on average per sample for melanoma, 39.22 (13.95%) on the liver, and 46.42 (12.35%) on lung cancer with average f-scores per sample respectively 87.88, 87.8 and 89.05. Both indels and proximal variants contribute to or create open reading frames that might be an ideal source of tumor-derived neoantigens and so induce multiple neoantigen reactive T cells [33].
From all observed mutational events phasing has the smallest, but still significant influence on both FEs (8.10 on melanoma, 8.35 on liver, and 8.16 on lung on average per sample) and FDs (3.73 on melanoma, 3.20 on liver, and 3.14 on lung cancer type on average per sample) and with the average per sample f-scores respectively 96.9, 95.1 and 96.5.
It is worth noticing that the number of FDs and FEs while ignoring the proximal variants has the largest fluctuation between samples - from 10 to 125 and neglecting indels has a large fluctuation of FEs (10 to 125) with f-scores spawning between samples from 60 to 97 (Figure 2b).
Another strong motivation for developing INAEME is to build an integral analysis for neoantigen discovery, starting from raw sequenced reads to neoantigen candidates with all important features that contribute to prioritizing and selecting the best ones. For that reason, each produced neoantigen candidate, besides peptide sequence and HLA type, contains features such as the information about the DNA somatic variant from which it originates including tumor and normal variant allele frequencies, MHC binding prediction scores (NetCTLPan, NetMHCPan, Pickpocket), agretopicity, RNA expression of the transcript from which is extracted, RNA variant and its allelic count. Additionally, neoantigen candidates present in wildtype protein databases, are optionally filtered out. All filtering parameters and settings are flexible and exposed in the CWL description of the workflow, making them easy to configure before starting the execution of the workflow.
Accurate, reproducible, and rapid discovery of neoantigen candidates represents a foundation for personalized cancer vaccine development. Paired with a cloud environment and integral analysis entirely described in CWL, INAEME workflow has the potential to fulfill the demands for rapid turnaround of accurate predictions within a clinically compliant environment for a large number of patients.

Methods

INAEME is described in Common Workflow Language [18] where all of the total 130 bioinformatics tools are executed inside corresponding Docker containers making it fully reproducible and portable to any computational platform. It is also highly configurable having a number of exposed parameters that enable simple comparison analysis and measuring of influence of certain settings. The execution flow of INAEME is similar to the general neoantigen discovery flow [20][21] with some additional processing steps (Figure 5).

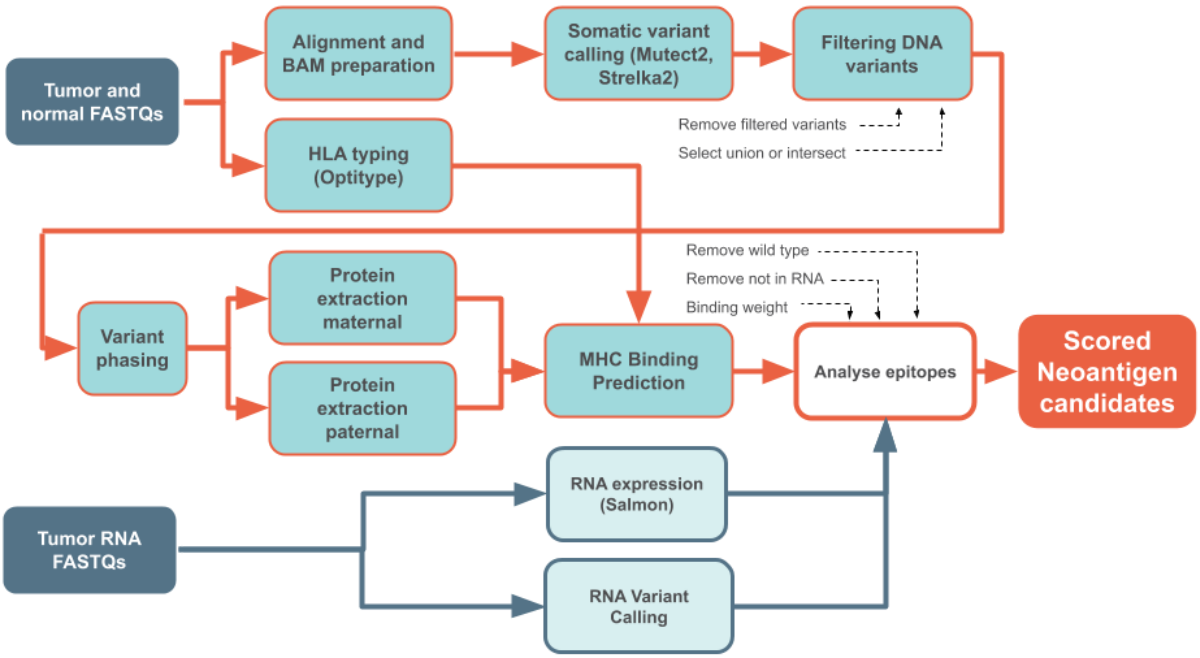

Figure 5: Detailed processing diagram of INAEME.

The first step performs read alignment [23], leveraging GATK best practices. Next, somatic variant calling using Mutect2 [24] and Strelka2 [25] is performed and variants are merged into one file. Merging is configurable and includes selecting intersect (default) or union of variants from these two callers. Once the somatic variants are merged, an optional and recommended step is variant phasing which identifies alleles on maternal and paternal chromosomes (Figure 1b) [26]. OptiType [27] calculates Human Leukocyte Antigen (HLA) types from tumor DNA FASTQs which will be later used for MHC binding prediction.
RNA transcript expression quantification is used to enable the selection of influential DNA variants that will be translated into proteins of interest. RNA reads are processed with Salmon and/or RSEM tools, which enable high-precision quantification of transcripts. The result of RNA expression analysis is a list of gene isoforms with corresponding RNA expression scores.
Also, RNA reads are used to call RNA variants with the GATK4 RNA Variant Calling workflow.
Once DNA, RNA, and HLA processing steps are finished, obtained data are used for the determination of potential neoantigens and their ranking based on HLA compatibility. To do so, phased somatic DNA variants, optionally filtered with RNA variants (if RNA data is available) to boost up the precision of neoantigen candidates, are passed to Protein Extraction Tools. This step consists of several custom-developed Python tools that perform the application of all variants to the reference genome and translation of the extracted nucleotide sequences around the somatic variants to proteins (neoantigen nests). The area around the altered amino acid that defines the neoantigen nest is configurable and set by default to 10 amino acids on both sides giving, for a single nucleotide variant total size of 21 amino acids. The area of 10 amino acids is chosen because the maximal peptide size for neoantigen candidates supported in our binding

prediction tools is 11. Protein Extraction Tools take into account the full range of above mentioned mutational events, currently not existent within the published neoantigen workflows, and also: changes from both germline and somatic variants (SNPs and indels), variants within the STOP codon (nonstop) and mutations that create STOP codons (nonsense). The extracted protein sequence and identified HLA type are used by the epitope prediction tools NetCTLpan [28], NetMHCpan [29], PickPocket [30] trained on peptides from the Immune Epitope Database (IEDB) [31] to compute confidence-ranked neoantigen candidates.

Finally, a list of the confidence-ranked neoantigen candidates with HLA types, variant information, RNA expression, and RNA variant calling scores are merged and prioritized in the Analyse epitopes tool. The final score on which neoantigen candidates are prioritized is configurable and by default calculated using a combination of normalized epitope binding score from the MHC binding prediction tool (selectable from the list of tools - NetCTLPan, NetMHCPan, Pickpocket) and normalized RNA expression. The weight parameter applicable to some of these two scores is also configurable. Our experiments conducted on samples from the Tesla challenges [19] with available sets of flow-cytometry validated neoantigen candidates showed that the weighting normalized MHC binding score with 0.7 and normalized RNA expression with 0.3 give the best final score (more trust is given to MHC-binding score). The transcript to which the DNA somatic variant falls can be highly expressed which would give neoantigen candidates originating from it a very high score, but this score is incorrect if the reference allele of the transcript is expressed and not the alternative (mutated) one. To mitigate this scenario we added a configurable possibility enabled by RNA variant calling to filter false positive neoantigen candidates originating from DNA variants that are not called in RNA. Measuring the influence of RNA variant calling on obtaining accurate neoantigen candidates is not considered in this paper and represents one of the targets for future works.

Agretopicity of neoantigen candidates is also one of the features calculated in the Analyse epitopes tool together with tumor and normal VAFs (variant allele frequencies). If a wild-type protein database is provided to Analyse epitopes it is possible to additionally filter neoantigen candidates that are identical to some wild-type protein. Also, neoantigen candidates containing three or more same amino acids in a row are filtered out by default. The Analyse epitopes tool produces the final report table with prioritized neoantigen candidates (peptide-HLA pair) and all above-mentioned features and scores for it (originating somatic DNA variant location, filter and info fields, scores from all MHC-binding tools, RNA expression, allelic depth and depth of originating RNA variant if called, tumor and normal VAFs, agretopicity, etc).

Data and code availability.

The INAEME workflow described in CWL is available for use in academic research projects without restrictions on the Cancer Genomics Cloud platform, while for commercial usage it requires the purchase of the license. The data used in this paper is available on The Cancer Genome Atlas (TCGA) database.

Acknowledgments

The authors thank Nikola Skundric for managing and organizing project resources, Ana Mijalkovic Lazic for initial discussion about the project, Milica Kojicic for testing protein extraction tools, Mladen Lazarevic, Brandi Davis-Dusenbery, Aleksandra Kovacevic, Nevena Veljkovic, Julie Gil and Jeffrey Brabec for reviewing the paper and providing useful comments.
The results published here are in whole or part based upon data generated by the TCGA Research Network: https://www.cancer.gov/tcga. dbGaP access for processing TCGA samples was enabled by the National Institutes (request #88805-1 for access phs000178/GRU, INC5023870).

Author contributions

V. B. K. was involved in all aspects of this study, including constructing and developing the methodology, analyzing and interpreting data, and writing the manuscript. N.I.R. was developing the RNA analysis part of the workflow and helped with the review of the paper. O. M. contributed to the development of the initial idea, methodology for variant translation, protein extraction, reviewing the paper, and visualizations.

Competing interests

The authors declare no competing interests.

References

1. Zitvogel, L., Tesniere, A. & Kroemer, G. Cancer despite 1: immunoselection and immunosubversion. Nat Rev Immunol 6, 715–727 (2006).
2. Marta Helena Kubala, Vasu Punj, Veronica Rae Placencio-Hickok, Plasminogen Activator Inhibitor-1 Promotes the Recruitment and Polarization of Macrophages in Cancer. Cell Reports, 25, 8, P2177-2191.E7 (2018).
3. Conor M. Henry et al. Caspase-8 Acts in a Non-enzymatic Role as a Scaffold for Assembly of a Pro-inflammatory “FADDosome” Complex upon TRAIL Stimulation. Molecular Cell, 65, 4, P715-729.E5, (2017)
4. Lang, F., Schrörs, B., Löwer, M. et al. Identification of neoantigens for individualized therapeutic cancer vaccines. Nat Rev Drug Discov 21, 261–282 (2022).
5. Jiang, T., Shi, T., Zhang, H. et al. Tumor neoantigens: from basic research to clinical applications. J Hematol Oncol 12, 93 (2019).
6. Ott, P., Hu, Z., Keskin, D. et al. An Immunogenic Personal Neoantigen Vaccine for Melanoma Patients. Nature 547, 217–221 (2017).
7. Sahin, U., Derhovanessian, E., Miller, M. et al. Personalized RNA mutanome vaccines mobilize poly-specific therapeutic immunity against cancer. Nature 547, 222–226 (2017).
8. Guo Y, Lei K, Tang L. Neoantigen Vaccine Delivery for Personalized Anticancer Immunotherapy. Front Immunol. 9:1499 (2018).
9. Hundal, J., Carreno, B.M., Petti, A.A. et al. pVAC-Seq: A genome-guided in silico approach to identifying tumor neoantigens. Genome Med 8, 11 (2016).
10. Preeti Bais et al. CloudNeo: a cloud pipeline for identifying patient-specific tumor neoantigens. Bioinformatics, 1, 33, 19 (2017).
11. Rubinsteyn A. et al. Computational Pipeline for the PGV-001 Neoantigen Vaccine Trial. Front. Immunol. 8:1807 (2018).
12. Hundal, J., Kiwala, S., Feng, Y. et al. Accounting for proximal variants improves neoantigen prediction. Nat Genet 51, 175–179 (2019).

13. Steven P Vensko, II, Kelly Olsen, Dante Bortone, Christof C Smith, Shengjie Chai, Wolfgang Beckabir, Misha Fini, Othmane Jadi, Alex Rubinsteyn, Benjamin G Vincent, LENS: Landscape of Effective Neoantigens Software, Bioinformatics, Volume 39, Issue 6 (2023).
14. Daniel Oreper, Susan Klaeger, Suchit Jhunjhunwala, Lélia Delamarr, The peptide woods are lovely, dark and deep: Hunting for novel cancer antigens, Seminars in Immunology, Volume 67 (2023).
15. Zhan Zhou a d 1, Jingcheng Wu a b 1, Jianan Ren a, Wenfan Chen a f, Wenyi Zhao a b, Xun Gu c, Ying Chi e, Qiaojun He a d, Bo Yang a d, Jian Wu b d g, Shuqing Chen, TSNAD v2.0: A one-stop software solution for tumor-specific neoantigen detection, Computational and Structural Biotechnology Journal, Volume 19 (2021).
16. Carolyn Hutter, Jean Claude Zenklusen, The Cancer Genome Atlas: Creating Lasting Value beyond Its Data, Cell, 173, 2, P283-285 (2018).
17. Jessica W. Lau et. al. The Cancer Genomics Cloud: Collaborative, Reproducible, and Democratized-A New Paradigm in Large-Scale Computational Research, Cancer Res 77, 21, e3-e6 (2017).
18. Peter Amstutz et al. Common Workflow Language, v1.0, 10.6084/m9.figshare.3115156.v2 (2016).
19. Daniel K. Wells et al. Key Parameters of Tumor Epitope Immunogenicity Revealed Through a Consortium Approach Improve Neoantigen Prediction, Cell, 183, 3, 818-834, October 2020.
20. Efremova M, Finotello F, Rieder D, and Trajanoski Z, Neoantigens Generated by Individual Mutations and Their Role in Cancer Immunity and Immunotherapy. Front. Immunol. 8:1679 (2017).
21. Marion Arnaud et al. Biotechnologies to tackle the challenge of neoantigen identification. Current Opinion in Biotechnology 65, 0958-1669 (2020).
22. Peng, M., Mo, Y., Wang, Y. et al. Neoantigen vaccine: an emerging tumor immunotherapy. Mol Cancer 18, 128 (2019).
23. Heng Li et al. Fast and accurate long-read alignment with Burrows–Wheeler transform. Bioinformatics 26, 589–595 (2010).
24. David Benjamin et al. Calling Somatic SNVs and Indels with Mutect2, Preprint from bioRxiv (2019).
25. Sangtae Kim, Konrad Scheffler, Aaron L. Halpern, Mitchell A. Bekritsky, Eunho Noh, Morten Källberg, Xiaoyu Chen, Yeonbin Kim, Doruk Beyter, Peter Krusche & Christopher T. Saunders, Strelka2: fast and accurate calling of germline and somatic variants, Nature Methods, Volume 15 (2018).
26. Castel, S., Mohammadi, P., Chung, W. et al. Rare variant phasing and haplotypic expression from RNA sequencing with phASER. Nat Commun 7, 12817 (2016).
27. Szolek, A. et al. OptiType: precision HLA typing from next-generation sequencing data. Bioinformatics 30, 3310–3316 (2014).
28. Stranzl, T., Larsen, M.V., Lundegaard, C. et al. NetCTLpan: pan-specific MHC class I pathway epitope predictions. Immunogenetics 62, 357–368 (2010).
29. Birkir Reynisson, Bruno Alvarez, Sinu Paul, Bjoern Peters, Morten Nielsen, NetMHCpan-4.1 and NetMHCIIpan-4.0: improved predictions of MHC antigen

presentation by concurrent motif deconvolution and integration of MS MHC eluted ligand data, Nucleic Acids Research, 48, W1 (2020).
30. Hao Zhang, Ole Lund, and Morten Nielsen, The PickPocket method for predicting binding specificities for receptors based on receptor pocket similarities: application to MHC-peptide binding, Bioinformatics. 15, 25, 10, 1293–1299 (2009).
31. Vita, R. et al. The immune epitope database (IEDB) 3.0. Nucleic Acids Res. 43, D405–D412 (2014).
32. Tanner M. Johanns et al. Detection of neoantigen-specific T cells following a personalized vaccine in a patient with glioblastoma. OncoImmunology, 8:4 (2019).
33. SamraTurajlic et al. Insertion-and-deletion-derived tumour-specific neoantigens and the immunogenic phenotype: a pan-cancer analysis. The Lancet Oncology, 18, 8 (2017).
34. Schumacher N. et al., Neoantigens in cancer immunotherapy. Science, 348, 6230, 69-74 (2015).

Supplementary

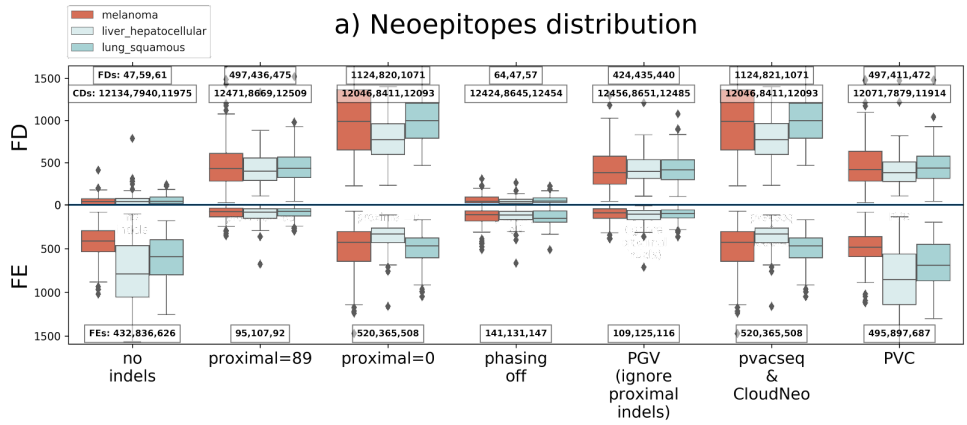

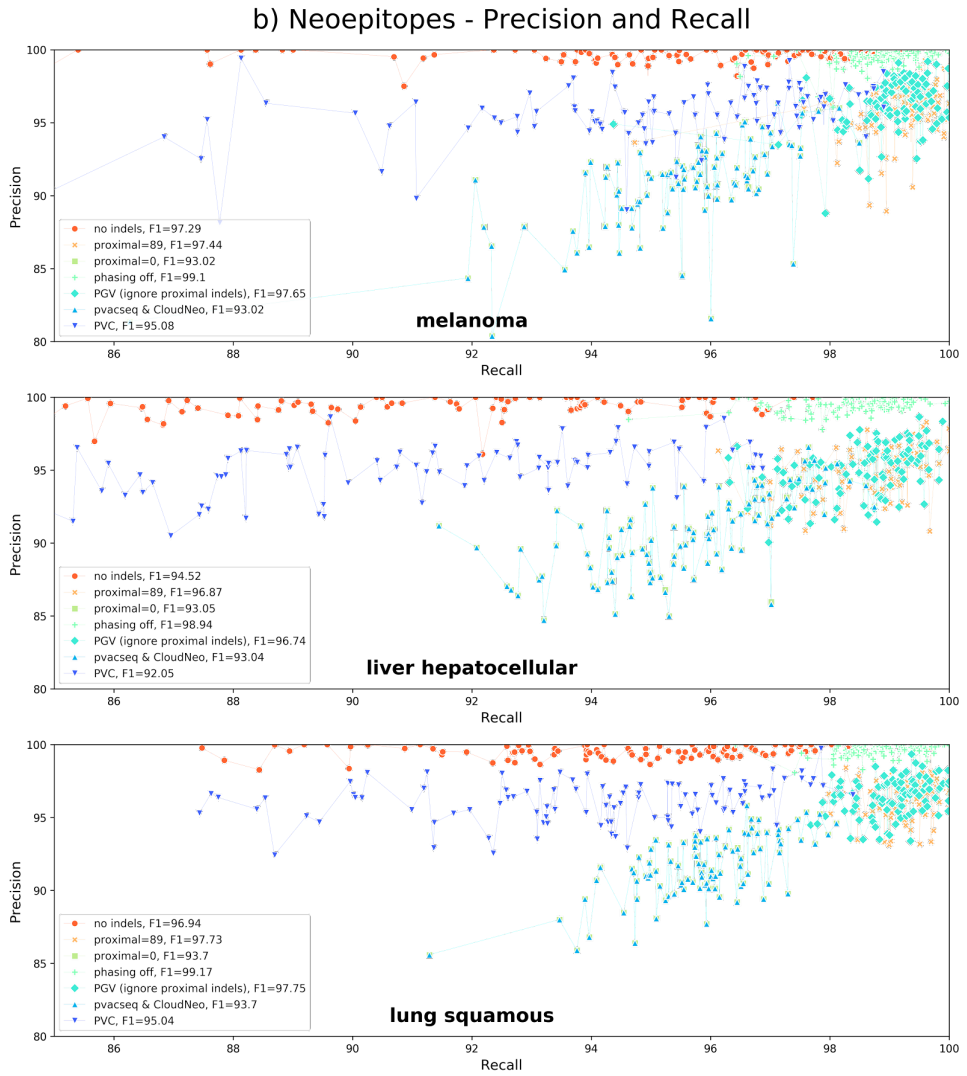

Figure 1: (a) Distribution of FDs, CDs, and FEs on neoepitopes across 100 samples of melanoma, hepatocellular carcinoma and lung squamous cancer, respectably, when some of the mutational events are switched off: all indels are ignored, the proximal area size of only 89 nucleotides as used in PVC, all proximal variants ignored (proximal=0), excluding variant phasing, the influence of indels around currently processed somatic variant (as excluded in PGV), pvacseq & CloudNeo (excluding phasing and proximal area equals 0) and PVC (no indels and proximal area of 89). Total numbers of FDs, FEs, and CDs are given in the boxes for each mutational event switch off and for each algorithm with its mutational events switched off. (b) Precision and recall scores on neoepitopes across 100 samples each of melanoma, hepatocellular carcinoma, and lung squamous cancer when the same mutational events are switched off. Mean f-scores (F1) across all samples when a mutational event is switched off are given in the figure's legend. Neoepitopes (sizes 8, 9, 10, and 11 amino acids) are spawned from all neoantigen nests not contained in the wild type protein database.

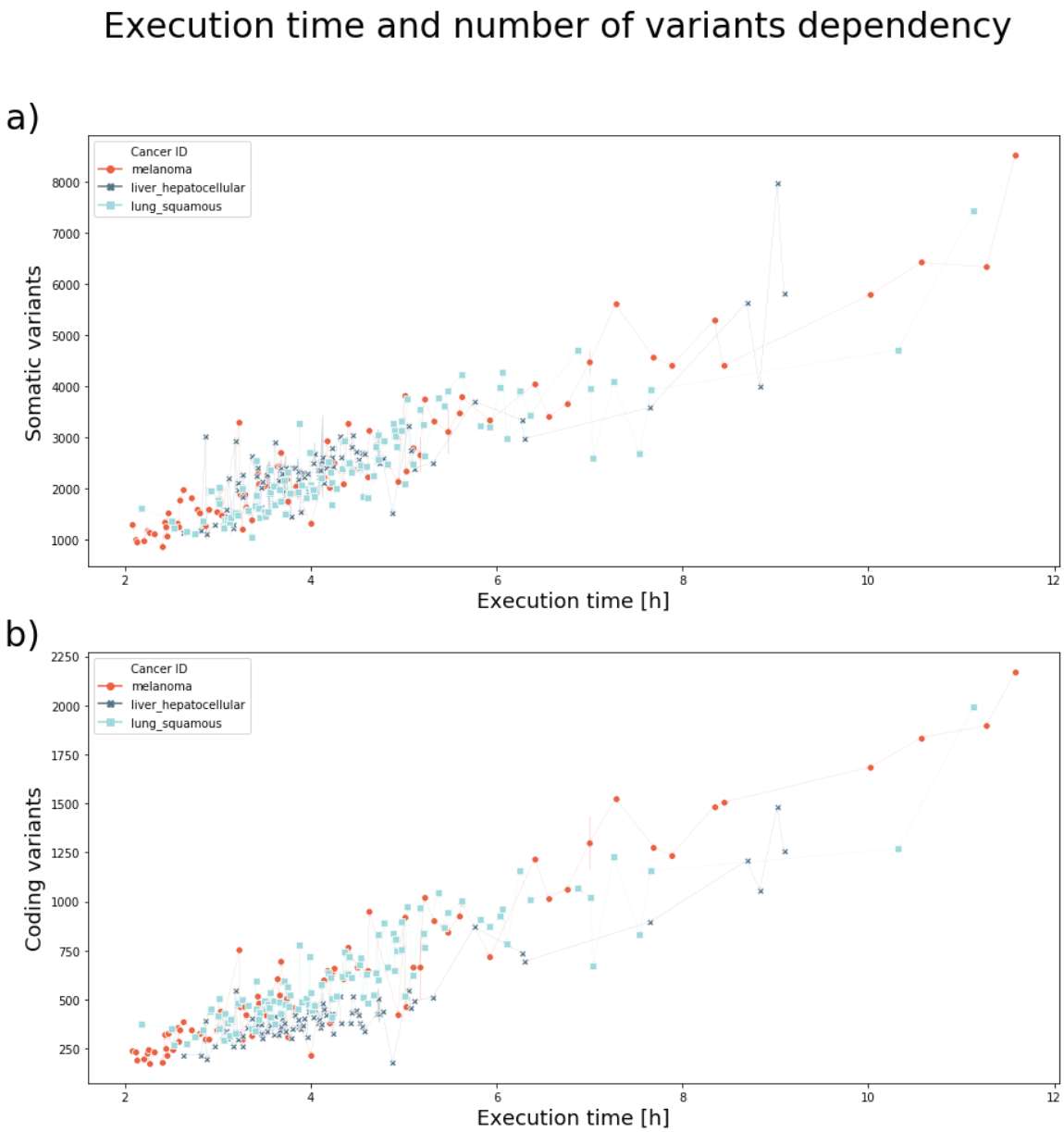

Figure 2: Distribution of INAEME execution times across 100 samples of melanoma, hepatocellular carcinoma and lung squamous cancer (total 300 samples). (a) Dependency of execution time and number of somatic variants detected in the sample. (b) Dependency of execution time and number of somatic variants that fall into gene coding regions.

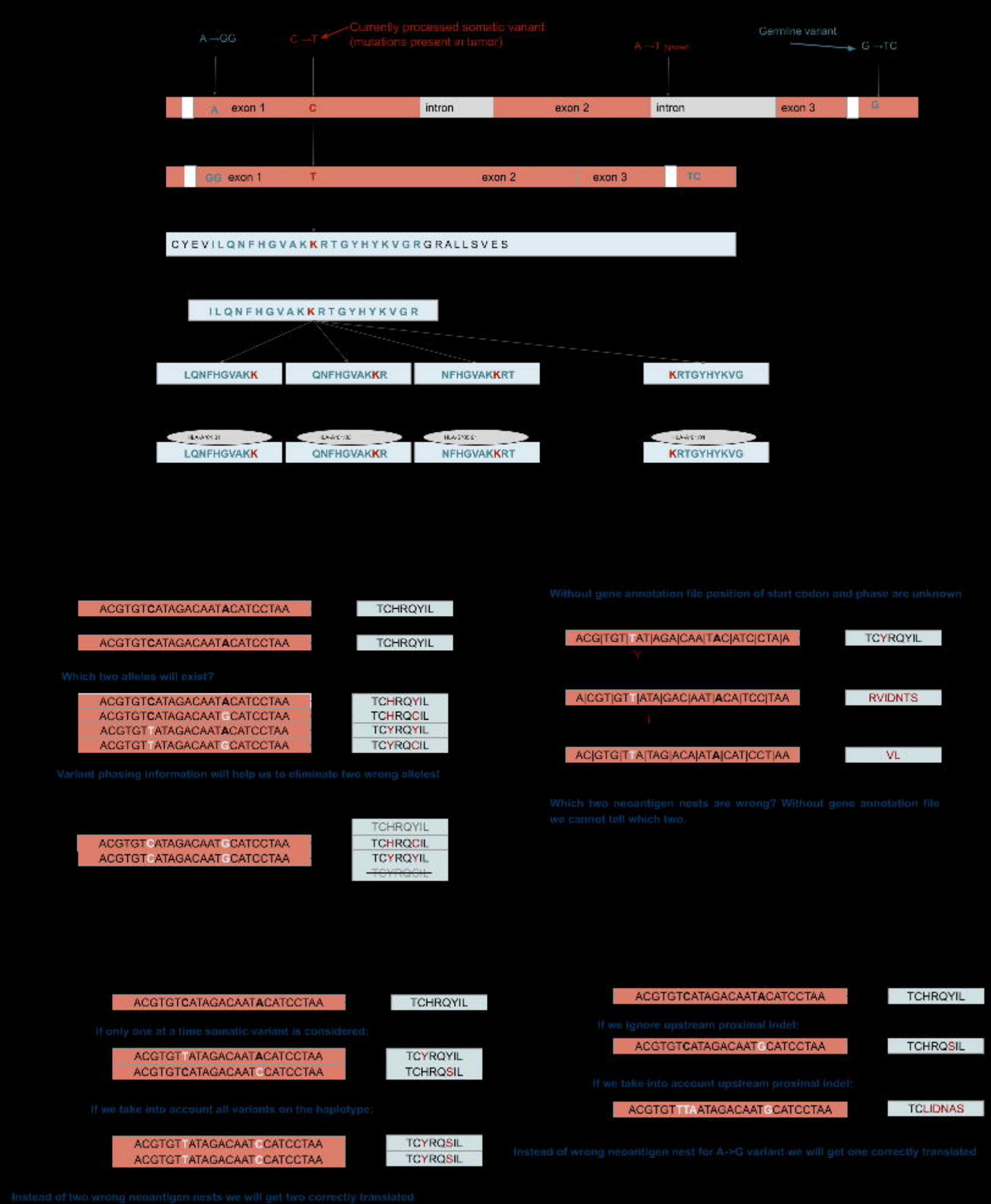
A→GG
C→T
Currently processed somatic variant
(mutations present in tumor)
A→T (phase)
Germline variant
G→TC
A exon 1 C intron exon 2 intron exon 3 G
GG exon 1 T exon 2 exon 3 TC
CYEVILQNFHGVAKKRTGYHYKVGRGRALLSVES
ILQNFHGVAKKRTGYHYKVGR
LQNFHGVAKK
QNFHGVAKKR
NFHGVAKKRT
KRTGYHYKVG
LQNFHGVAKK
QNFHGVAKKR
NFHGVAKKRT
KRTGYHYKVG
ACGTGTCATAGACAATACATCCTAA
TCHRQYIL
ACGTGTCATAGACAATACATCCTAA
TCHRQYIL
Which two alleles will exist?
ACGTGTCATAGACAATACATCCTAA
ACGTGTCATAGACAATGCATCCTAA
ACGTGTTATAGACAATACATCCTAA
ACGTGTTATAGACAATGCATCCTAA
TCHRQYIL
TCHRQCIL
TCYRQYIL
TCYRQCIL
Variant phasing information will help us to eliminate two wrong alleles!
ACGTGTCATAGACAATGCATCCTAA
ACGTGTCATAGACAATGCATCCTAA
TCHRQYIL
TCHRQCIL
TCYRQYIL
TCYRQCIL
Without gene annotation file position of start codon and phase are unknown
ACG|TGT|TAT|AGA|CAA|TAC|ATC|CTA|A
Y
TCYRQYIL
A|CGT|GTT|ATA|GAC|AAT|ACA|TCC|TAA
I
RVIDNTS
AC|GTG|TTA|TAG|ACA|ATA|CAT|CCT|AA
VL
Which two neoantigen nests are wrong? Without gene annotation file we cannot tell which two.
ACGTGTCATAGACAATACATCCTAA
TCHRQYIL
If only one at a time somatic variant is considered:
ACGTGTTATAGACAATACATCCTAA
ACGTGTCATAGACAATCCATCCTAA
TCYRQYIL
TCHRQSIL
If we take into account all variants on the haplotype:
ACGTGTTATAGACAATCCATCCTAA
ACGTGTTATAGACAATGCATCCTAA
TCYRQSIL
TCYRQSIL
Instead of two wrong neoantigen nests we will get two correctly translated
ACGTGTCATAGACAATACATCCTAA
TCHRQYIL
If we ignore upstream proximal indel:
ACGTGTCATAGACAATGCATCCTAA
TCHRQSIL
If we take into account upstream proximal indel:
ACGTGTTTAATAGACAATGCATCCTAA
TCLIDNAS
Instead of wrong neoantigen nest for A->G variant we will get one correctly translated

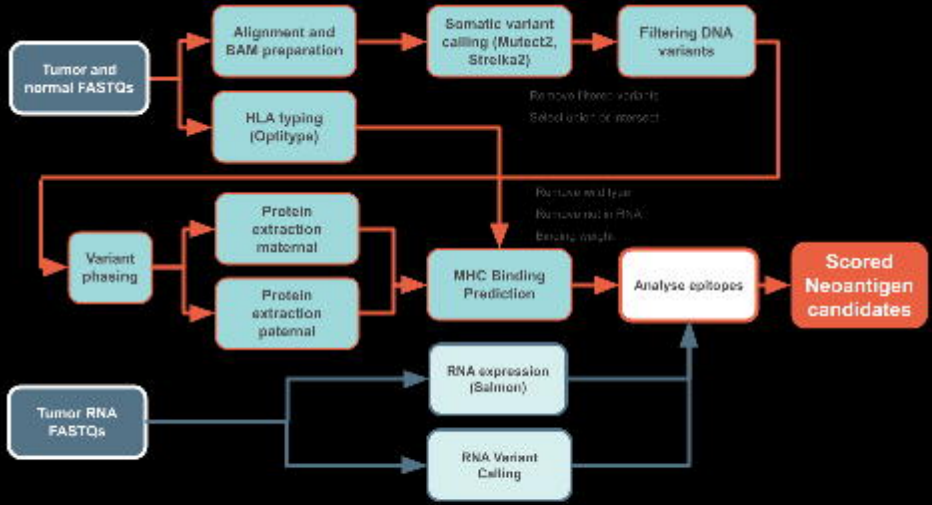
Tumor and normal FASTQs
Alignment and BAM preparation
Somatic variant calling (Mutect2, Strelka2)
Filtering DNA variants
HLA typing (Optitype)
Variant phasing
Protein extraction maternal
Protein extraction paternal
MHC Binding Prediction
Analyse epitopes
Scored Neoantigen candidates
Tumor RNA FASTQs
RNA expression (Salmon)
RNA Variant Calling

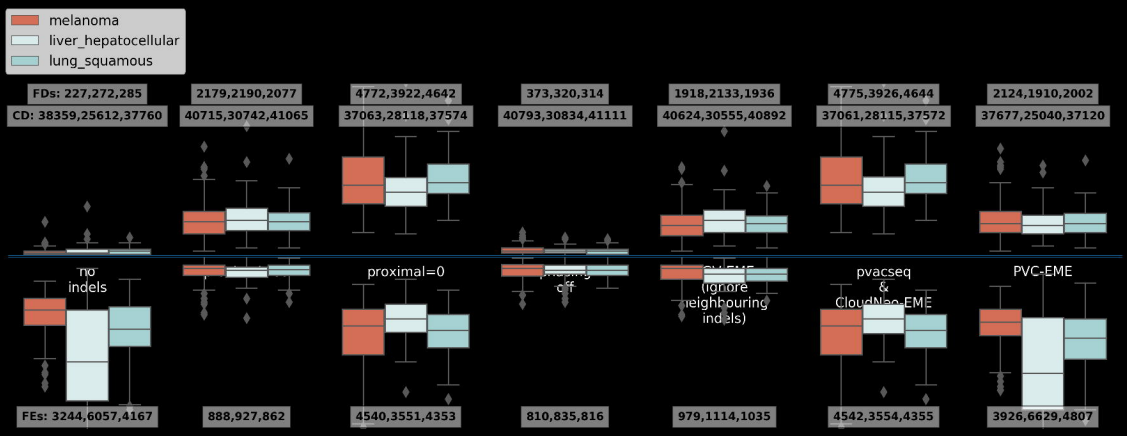
melanoma
liver_hepatocellular
lung_squamous
FDs: 227,272,285
CD: 38359,25612,37760
2179,2190,2077
40715,30742,41065
4772,3922,4642
37063,28118,37574
373,320,314
40793,30834,41111
1918,2133,1936
40624,30555,40892
4775,3926,4644
37061,28115,37572
2124,1910,2002
37677,25040,37120
no indels
proximal=0
pvacseq & CloudNeo-EME
PVC-EME
FEs: 3244,6057,4167
888,927,862
4540,3551,4353
810,835,816
979,1114,1035
4542,3554,4355
3926,6629,4807

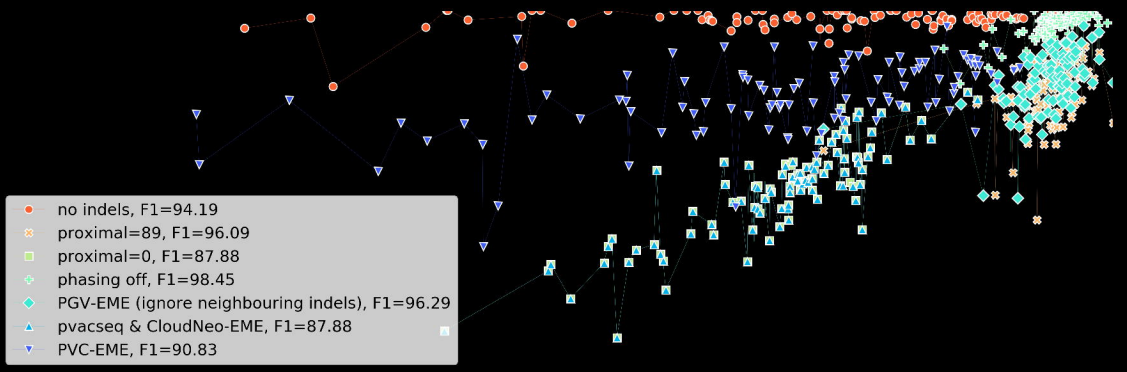
no indels, F1=94.19
proximal=89, F1=96.09
proximal=0, F1=87.88
phasing off, F1=98.45
PGV-EME (ignore neighbouring indels), F1=96.29
pvacseq & CloudNeo-EME, F1=87.88
PVC-EME, F1=90.83

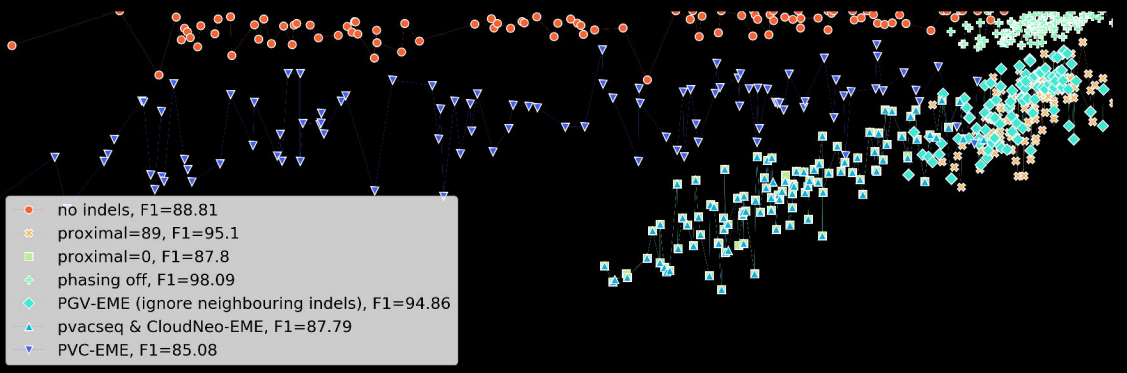
no indels, F1=88.81
proximal=89, F1=95.1
proximal=0, F1=87.8
phasing off, F1=98.09
PGV-EME (ignore neighbouring indels), F1=94.86
pvacseq & CloudNeo-EME, F1=87.79
PVC-EME, F1=85.08

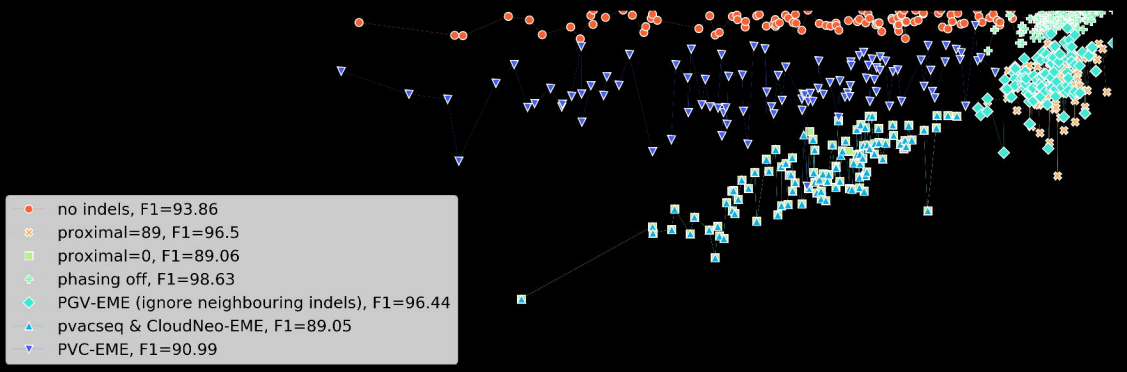
no indels, F1=93.86
proximal=89, F1=96.5
proximal=0, F1=89.06
phasing off, F1=98.63
PGV-EME (ignore neighbouring indels), F1=96.44
pvacseq & CloudNeo-EME, F1=89.05
PVC-EME, F1=90.99

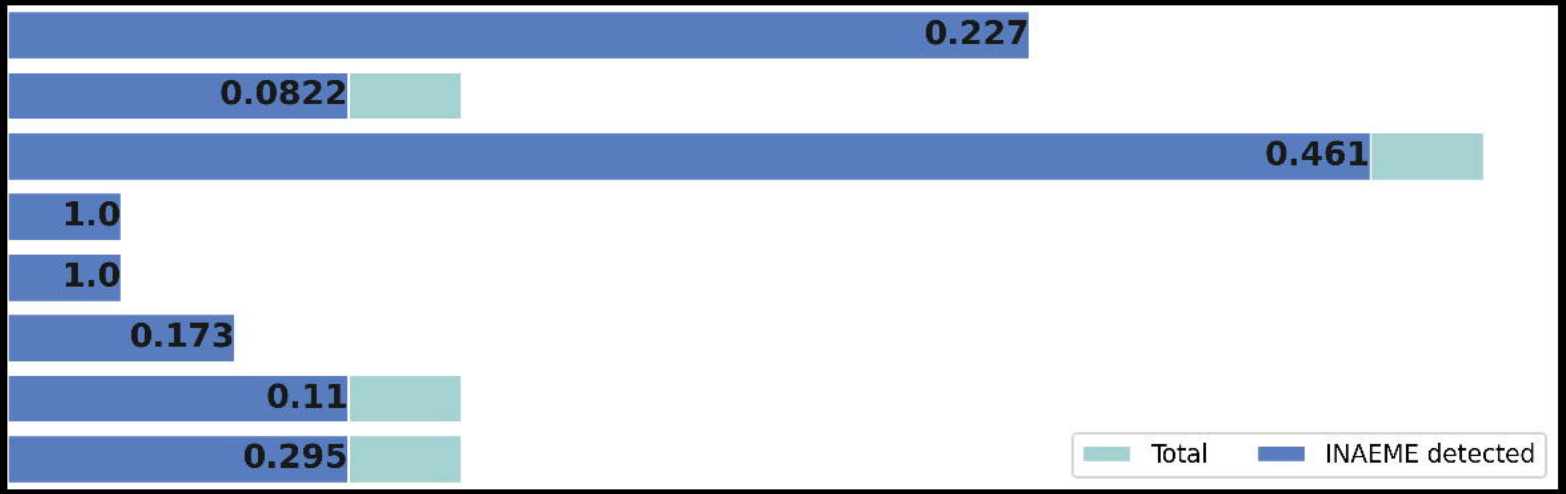
0.227
0.0822
0.461
1.0
1.0
0.173
0.11
0.295
Total
INAEME detected

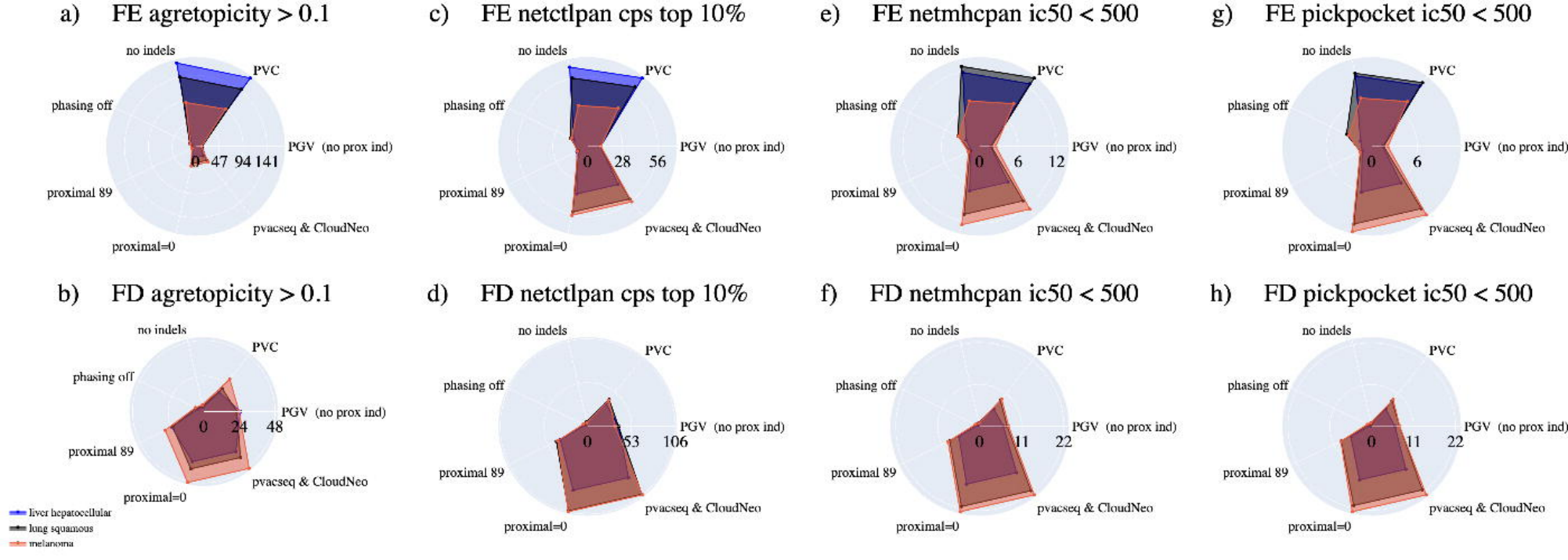
a) FE agretopicity > 0.1
no indels
PVC
phasing off
PGV (no prox ind)
0 47 94 141
proximal 89
pvacseq & CloudNeo
proximal=0
b) FD agretopicity > 0.1
no indels
PVC
phasing off
PGV (no prox ind)
0 24 48
proximal 89
pvacseq & CloudNeo
proximal=0
c) FE netctlpan cps top 10%
no indels
PVC
phasing off
PGV (no prox ind)
0 28 56
proximal 89
pvacseq & CloudNeo
proximal=0
d) FD netctlpan cps top 10%
no indels
PVC
phasing off
PGV (no prox ind)
0 53 106
proximal 89
pvacseq & CloudNeo
proximal=0
e) FE netmhcpan ic50 < 500
no indels
PVC
phasing off
PGV (no prox ind)
0 6 12
proximal 89
pvacseq & CloudNeo
proximal=0
f) FD netmhcpan ic50 < 500
no indels
PVC
phasing off
PGV (no prox ind)
0 11 22
proximal 89
pvacseq & CloudNeo
proximal=0
g) FE pickpocket ic50 < 500
no indels
PVC
phasing off
PGV (no prox ind)
0 6
proximal 89
pvacseq & CloudNeo
proximal=0
h) FD pickpocket ic50 < 500
no indels
PVC
phasing off
PGV (no prox ind)
0 11 22
proximal 89
pvacseq & CloudNeo
proximal=0
liver hepatocellular
lung squamous
melanoma